

ARTICLE

Development of Gelatin-Based Active Packaging and Its Application in Bread Preservation

Hui Zheng^{1,2}, Xiaohan Chen², Li Li², Dawei Qi¹, Jiale Wang¹, Jiaying Lou^{1,*} and Wenjun Wang^{1,*}

¹Shanghai Tobacco Group Co., Ltd., Shanghai, 200082, China

²College of Food Science and Technology, Shanghai Ocean University, Shanghai, 201306, China

*Corresponding Authors: Jiaying Lou. Email: loujy@sh.tobacco.com.cn; Wenjun Wang. Email: wjwang2022@126.com

Received: 13 November 2022 Accepted: 03 January 2023 Published: 10 August 2023

ABSTRACT

The issue of plastic pollution has attracted widespread social attention. Gelatin is valued as a degradable bio-based material, especially as an edible active packaging material. However, the commonly used solution-casting film-forming technology limits the mass production of gelatin films. In order to improve the production efficiency and enhance the commercial value of gelatin films, in this study, fish gelatin (FG) particles were successfully blended with essential oils (EOs) to prepare active films by melt extrusion technique, a common method for commercial plastics, and applied to bread preservation. FG and EOs showed good compatibility with each other. The elongation at break was enhanced in all samples of films containing EOs. The addition of EOs weakened the oxygen barrier properties of the FG films. The gelatin films containing clove EO showed the highest DPPH radical scavenging rate of 39.38%. The films containing oregano EO showed the highest antibacterial activity, with 98.84% and 99.86% against *S. aureus* and *E. coli*, respectively. The bread preservation results showed a slower microbial growth rate in the samples preserved by the active films. The bread samples preserved in commercial PE film showed mold on day 3, and the bread samples preserved in active gelatin film showed mold visible to the naked eye by day 7. This study demonstrates the potential of gelatin-based activated films for commercial application in baked goods preservation.

KEYWORDS

Fish gelatin film; essential oils; melt extrusion; bread preservation

1 Introduction

Bioplastics come from renewable sources, and they are biodegradable. Reducing the production cost and increasing the yield of bioplastics are pressing issues today. The selection of suitable processing waste as a raw material for bioplastic production has become an effective means to reduce the cost of bioplastics. Films prepared from bioplastics could reduce consumers' dependence on petroleum-based packaging and play an essential role in achieving a circular economy and alleviating environmental pollution problems [1]. Bioplastic films can be made from natural polymers, such as proteins, polysaccharides, and lipids [2].

Gelatin is a water-soluble protein formed by partial or complete hydrolysis of collagen. Approximately 98.5% of the world's commercial gelatin is extracted from porcine and bovine hoof tissue [3]. However, mammals, such as pigs and cattle, may carry viruses, such as avian influenza, bovine spongiform



encephalopathy, and foot-and-mouth disease, thus posing a risk of spreading public health diseases. In addition, pork products are related to the religious beliefs of Muslim and Jewish countries and communities, and all pork-related products are subject to restrictions [4]. Fish gelatin (FG) has comparable functional properties to mammalian gelatin and could be a good substitute for it. FG can be extracted from various sources, including fish skin, scales, swim bladders, and cartilage. About 30% of fish processing waste is often used for gelatin extraction due to its collagen content [5]. FG has outstanding film-forming capabilities and oxygen barrier properties, rendering it a potential candidate for food packaging applications [6].

Simple operation and low equipment requirements of solution casting have made it the mainstream gelatin film preparation process. However, the low productivity of this method makes it challenging to meet the demand for commercial applications. Single-component gelatin film is brittle and contains many polar groups, which are highly sensitive to moisture and likely to swell, dissolve, or decompose when exposed to water, thereby limiting the application of gelatin film in high-humidity environments. In previous studies, FG film was successfully developed by melt extrusion, a typical commercial plastic method. Such a method dramatically increased the efficiency of gelatin film production. In addition, the premixing of FG particles with plasticizers (glycerol and water) and crosslinkers [transglutaminase (TGase) and beeswax (BW)] resulted in enhanced mechanical and moisture-sensitive properties [7]. Notably, FG almost has no antibacterial properties. Adding active substances to the formulation of FG composite film could prevent it from mold. In addition, the migration and release of active substances from the film matrix into the food could inhibit the growth and reproduction of microorganisms on the food surface, thus extending the shelf life of the food [2].

Essential oils (EOs), considered safe biological additives by the Food and Drug Administration (FDA), are oil-like plant secondary metabolites with good antibacterial and antioxidant properties. Clove has a long history as a traditional natural medicinal plant in China. Clove EO (CEO) is widely used in food, cosmetics, pharmaceuticals, and active packaging due to the content of its various active ingredients, such as clove phenol and caryophyllene [8]. Liu et al. [9] found that the edible coating containing CEO could maintain the quality of white prawn shrimp during storage. Tea tree oil (TTO) is mainly extracted from the roots, stems, leaves, and other tissues of tea trees and is transparent yellow. TTO has sound antibacterial and anti-inflammatory effects, and it could be applied to active packaging to extend the shelf life of food. Yang et al. [10] prepared active packaging by co-blending nano-emulsion containing TTO with sodium alginate/TiO₂ film-forming solution and applied it to banana preservation. The film effectively maintained the post-harvest quality of bananas and reduced the incidence of anthracnose. Oregano is a common herb widespread in the Mediterranean and Asian regions. Carvacrol can make up 93.58% of oregano essential oil (OEO) and is its primary antibacterial and antioxidant component [11]. Yang et al. [12] preserved salmon fillets using PLA-PBSA films containing carvacrol, resulting in a 3–4-day shelf life extension.

Bread is one of the most commonly consumed foods around the world. According to statistics, the annual bread consumption worldwide is up to 9 billion kg [13]. Fresh bread is rich in nutritional value and has high water activity, which is a natural medium for microbes [14]. The shelf life of bread without added preservatives is usually only 3–5 days [15]. The microorganisms in bread, especially molds, proliferate during storage, resulting in an undesirable appearance on the bread surface. In addition, the microbial growth in bread is a significant cause of off-flavors and fungal toxins, which may pose a threat to public health and cause significant damage to the baking industry and consumers [15].

However, there are few reports on melt extrusion for developing fish gelatin-based active films and even fewer studies on the application of fish gelatin films prepared by melt extrusion for food preservation. This study aimed to prepare FG-based films by melt extrusion. In addition, EOs were added to the base formulation to enhance the application potential of the films. The films were measured for microstructure,

thermal stability, mechanical properties, barrier properties, water sensitivity, antioxidant properties, and antibacterial properties to evaluate the effect of EOs on the performance of extruded FG-based films. The prepared films were applied to bread preservation to investigate the effect of FG-based active films on the shelf life of bread.

2 Materials and Methods

2.1 Materials

Tilapia-scale gelatin (250 bloom value) was provided by Oudima Biological Engineering Co., Ltd. (Guangdong, China). BW was bought from Changxing Bee Industry Co., Ltd. (Henan, China). TGase was bought from Yuantai Bioengineering Co., Ltd. (Shandong, China). Glycerin was purchased from Titan Scientific Co., Ltd. (Shanghai, China). TWEEN 80 was acquired from Sinopharm Chemical Reagent Co., Ltd. (Shanghai, China). CEO, TTO, and OEO were obtained from Zhongxiang Natural Plant Co., Ltd. (Jiangxi, China). 2,2-Diphenyl-1-picrylhydrazyl (DPPH) was obtained from Macklin Biochemical Co., Ltd. (Shanghai, China). *S. aureus* (ATCC 6538) and *E. coli* (CMCC 8099) were kindly provided by Luwei Technology Co., Ltd. (Shanghai, China). Breadmaking materials were purchased from the T-mall online supermarket.

2.2 Film Preparation

In previous work, the best overall performance of the film was obtained when FG particles were blended with 5% BW and 1% TGase [7]. In the present study, the preparation process of FG active films was based on the best previous formulation, with slight modifications. First, a 5% BW (w/w, based on FG mass) emulsion and 1% TGase (w/w, based on FG mass) solution was prepared and blended with FG particles. The sealed modified gelatin particles were stored in an oven at 45°C for 4 h and then transferred to a refrigerator at 4°C for backup. As shown in Fig. 1, the modified FG particles were melted and extruded using a twin-screw extruder (Kechuang Equipment Co., Ltd., Shanghai, China). The temperature of the seven heating zones of the screw was set to 80°C, 90°C, 90°C, 100°C, 95°C, 85°C, and 80°C, and the screw speed was 125 rpm. The material extruded from the die mouth of the twin-screw extruder was pelletized after natural cooling. The pelletized samples were divided into four equal parts in accordance with mass, and three of them were randomly selected to be added with 5% (w/w, based on FG mass) CEO, TTO, and OEO separately. The samples were labeled as FG-BW-TGase, FG-BW-TGase-CEO, FG-BW-TGase-TTO, and FG-BW-TGase-OEO in accordance with their formulation composition. The four samples were melted again by a twin-screw extruder and then pelletized. The secondary pelletized samples were cast in a single-screw extruder (Jinzhonghe Machinery Co., Ltd., Foshan, China) with five heating zones set at 80°C, 90°C, 95°C, 105°C, and 105°C and a screw speed of 40 rpm. All films were conditioned at 25°C ± 2°C and 55% ± 5% RH for at least 24 h prior to index testing.

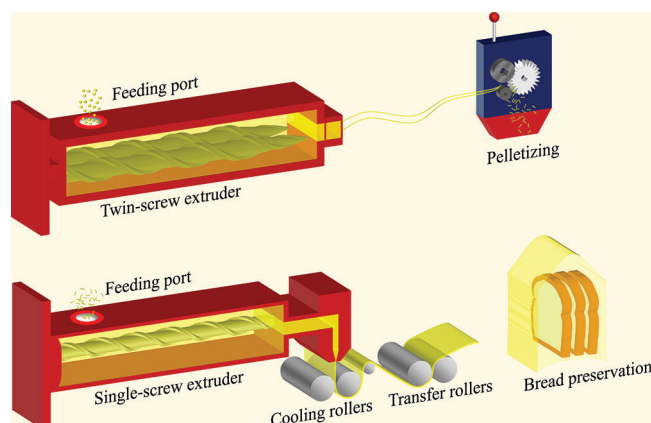


Figure 1: Preparation of FG-based film by melt extrusion and its application in bread preservation

2.3 Film Characterization

2.3.1 Scanning Electron Microscopy (SEM) and Fourier Transform Infrared (FTIR) Spectroscopy

The surface of the gelatin films was observed by SEM (Phenom XL, The Netherlands). In order to increase the films' electrical conductivity, the samples need to be coated with gold for 60 s. The surface structure of the gelatin films was observed at an accelerating voltage of 15 kV [16].

The FTIR variations of the films were mainly detected by FTIR spectrophotometer. The optical changes in the thin film samples were observed in the wavenumber range of 4,000–500 cm^{-1} . The scan times were set to 64, and the air spectrum was corrected for the background [17].

2.3.2 Differential Scanning Calorimetry (DSC)

The thermodynamic properties of the films were tested with a simple modification of the method of Ahammed et al. [17]. The aluminum crucible was sealed with a lid after placing 4–5 mg of the film sample. The sample was then placed in the instrument for two consecutive thermal scans. It was heated at a rate of 5°C/min from 0°C to 200°C and then, with the same heat exchange rate, cooled. The second thermal scan was performed with the same experimental parameters as the first one. Melting temperature (T_m) denotes the peak of the first temperature rise curve. Glass transition temperature (T_g) refers to the midpoint of the temperature jump change in the second heating curve.

2.3.3 Mechanical Properties

The film's tensile strength (TS) and elongation at break (EAB) were obtained by the XLW (EC) intelligent electronic stretching machine, with a testing process that complies with ASTM D882-12 (2012) [18]. The initial distance between the machine clamps was 60 mm, and the stretching speed was 50 mm/min. The size of the film was unified to 100 mm \times 15 mm.

2.3.4 Oxygen Transmission Rate (OTR)

The test process for the OTR of films was performed following ASTM D1434-82 (2015) [19]. The film samples were cut to uniform size by a film cutter and sealed in a gas permeation chamber. The environmental conditions of the chamber were 23°C and 50% RH. The specific test method referred to Jiang et al. [20].

2.3.5 Water Vapor Permeability (WVP)

The WVP of the films was measured following ASTM E96/E96M-16 (2016) [21]. A film cutter was used to cut the film into standard circles with a diameter of 80 mm. The circular films were then placed in a sealed water vapor permeability cup for testing. The specific machine parameters referred to Zheng et al. [7].

2.3.6 Moisture Content (MC) and Water Solubility (WS)

The results of MC and WS were obtained with simple modifications based on the method of Ahammed et al. [17]. Film samples were cut to a uniform size of 3 cm \times 3 cm, and the film mass was recorded as M_1 . The samples were dried in an oven at 105°C to a constant weight. The mass of the film after drying was recorded as M_2 . The MC of the film was calculated using Eq. (1).

$$MC(\%) = \frac{(M_1 - M_2)}{M_1} \times 100 \quad (1)$$

The dried film samples were soaked in 30 mL distilled water for 10 h and then placed in a magnetic mixer for 2 h at 200 rpm to dissolve the soluble material in the samples. The undissolved samples were transferred to a centrifuge for 10 min at 5000 rpm. The undissolved components were recovered and dried in an oven at 105°C to a constant weight. The difference in mass before and after was calculated. The film's WS was expressed as a percentage of the reduced mass to the dry film mass.

2.3.7 Water Contact Angle (WCA)

The WCA of the film was acquired by referring to the method of Chen et al. [22]. The film samples were laid on a contact angle tester table flat. The software on the device was used to capture the shape of the water droplet when the film first came in contact with 3 μL of distilled water. A five-point fit method was used to determine the contact angle of the film with the water droplet.

2.3.8 Antioxidation Performance Test

The antioxidant test of active films was a simple modification of the method of Liu et al. [23]. A 25 mg film sample was weighed, placed in 5 mL distilled water, and shaken with ultrasound for 30 min. Then, 0.1 mL of film extract was reacted with 3.9 mL of DPPH solution (0.1 mM ethanol solution) for 60 min while being protected from light, and then the absorbance of the solution at 517 nm was measured by a spectrophotometer. The DPPH radical scavenging activity of the films was calculated by Eq. (2).

$$DPPH_{\text{scavenging activity}}(\%) = 100 \times \left(1 - \frac{A_{\text{sample}}}{A_{DPPH}} \right) \quad (2)$$

where A_{DPPH} represents the absorbance of the control, and A_{sample} represents the absorbance of the sample.

2.3.9 Antimicrobial Performance Test

The antimicrobial properties of the composite films were simply modified from the work of Cui et al. [24]. Typical Gram-positive bacteria *S. aureus* and Gram-negative bacteria *E. coli* were selected for the study. The film inhibition ability was evaluated by the colony counting method. First, 100 μL of *S. aureus* and *E. coli* were inoculated in 10 mL of TSB medium. Then, the concentration of the bacterial solution was adjusted to 10^5 CFU/mL with saline, and 0.5 g of film sample was added to the diluted bacterial solution and incubated in a shaker at 37°C for 3 h. Subsequently, 1 mL of diluted bacterial solution and 15 mL of nutrient agar were added to the sterile plates, and then the plates were incubated in an incubator at 37°C for 24 h. Next, the bacterial count of the plates was recorded. The film inhibition rate was calculated using Eq. (3).

$$X(\%) = \frac{A - B}{A} \times 100 \quad (3)$$

where X is the inhibition rate (%), A is the number of colonies in the control gelatin film, and B is the number of colonies in the active gelatin film.

2.4 Experiment on the Preservation of Bread

2.4.1 Bread Making

High-gluten flour (1500 g), water (870 g), sugar (240 g), yeast (15 g), and salt (15 g) were placed into the mixer. The mixer parameters were set to 120 (4 min)–180 (4 min)–120 (4 min) rpm. When the dough could be pulled into a coarse film, 150 g of softened butter was added and mixing was continued. The mixer parameters were set as follows: 120 (4 min)–150 (2 min)–180 (4 min)–120 (2 min) rpm. The mixed dough was placed in a fermenter at 28°C and 75% RH for 50 min. Then, 450 g of fermented dough was placed in a mold, and a secondary fermentation was started at 34°C and 85% RH for 70 min. The fermented dough was transferred to the oven at 170°C and baked for 25 min. After the bread had cooled naturally, the bread was cut into 15 mm-wide slices. Then, the slices were trimmed with scissors to $80 \text{ mm} \times 80 \text{ mm} \times 15 \text{ mm}$. The bread slices were wrapped in commercially available polyethylene film and FG composite film. The packaged bread was stored at $26^\circ\text{C} \pm 1^\circ\text{C}$ and $75\% \pm 3\%$ RH and periodically tested for various indicators.

2.4.2 Moisture Distribution of Bread

The water distribution of the bread was based on the method of Zhou et al. [25]. The LF-NMR analyzer was used to obtain transverse relaxation T_2 profiles. The selected probe was MesoMR23-060H-I-70 mm. The proton resonance frequency was 21 MHz.

2.4.3 Textural Characterization of Bread

The texture of bread was characterized in accordance with the method of Ju et al. [26]. The bread slices were cut into rectangular squares of 20 mm × 20 mm × 15 mm. The P/36R cylindrical flat-bottom probe was selected for testing. The specific experimental parameters were as follows: trigger force of 5 g, pretest speed of 1 mm/s, test speed and posttest speed of 3 mm/s, sample compression deformation of 50%, and two compression intervals of 5 s.

2.4.4 Microorganism Changes in Bread

The microorganism changes in bread were examined according to Srisa et al. [27] with some modifications. A 15 g bread sample was homogenized with 135 mL saline and serially diluted in a gradient. Then, 1 mL of the bacterial solution was mixed with 15 mL of nutrient agar medium and then incubated at $37^\circ\text{C} \pm 1^\circ\text{C}$ for 48 ± 2 h, and the total number of colonies in the plate was recorded. The growth of mold and yeast was observed in the incubator at $28^\circ\text{C} \pm 1^\circ\text{C}$ for 5 days after 1 mL of bacterial solution was mixed with 15 mL of potato dextrose agar medium.

2.5 Statistical Analysis

ANOVA was performed using SPSS 26, and Duncan's test was selected for significance analysis ($p < 0.05$). Data were presented as mean \pm standard deviation of least three replicates, and Origin 2018 software was used for analysis and graphing.

3 Results and Discussion

3.1 Characterization of FG Active Films

3.1.1 SEM and FTIR

SEM was used to analyze the effect of EO incorporation on the microstructure of the gelatin-based composite films. As shown in Fig. 2, the surface of the control FG-BW-TGase films showed unevenly distributed bumps of different sizes. The surface of the EO-doped films was dense, flat, and uniform. The excellent biocompatibility of gelatin allowed the EO molecules to be uniformly dispersed in the gelatin matrix, and the crosslinking between EOs and protein could improve the surface properties of the films.

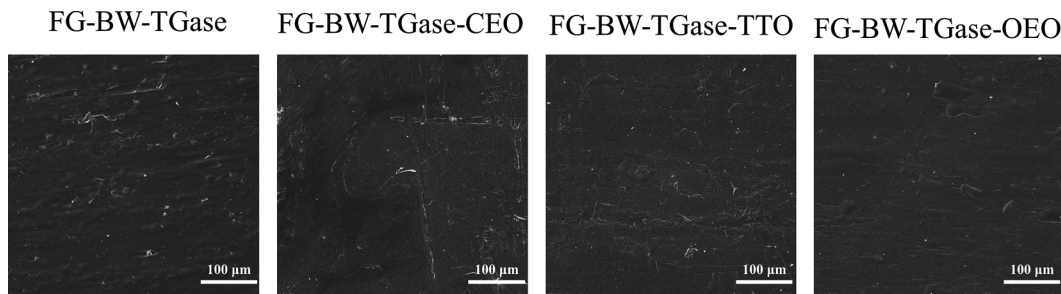


Figure 2: Microstructure of FG-based films

FTIR could reflect the interactions between the EOs of the gelatin polymer network. As shown in Fig. 3, all gelatin composite films showed peaks at 3280, 1629, 1542, and 1238 cm^{-1} , which are typical characteristic peaks of gelatin films, corresponding to amides A and I–III regions, respectively [17]. The

peaks formed at around 2917 and 2850 cm^{-1} in the composite films could be mainly attributed to the methylene asymmetry and symmetric stretching vibrations of the C-H group in BW [28]. The peak at 1033 cm^{-1} represented the interaction between the gelatin molecule and the O-H group in glycerol [29]. Moreover, no significant changes in the functional groups in the active FG composite films were observed, indicating that the addition of EOs did not change the structure of fish gelatin. However, the intensity of some peaks in the active composite films increased due to hydrogen bonding and van der Waals interactions between FG and EOs [30].

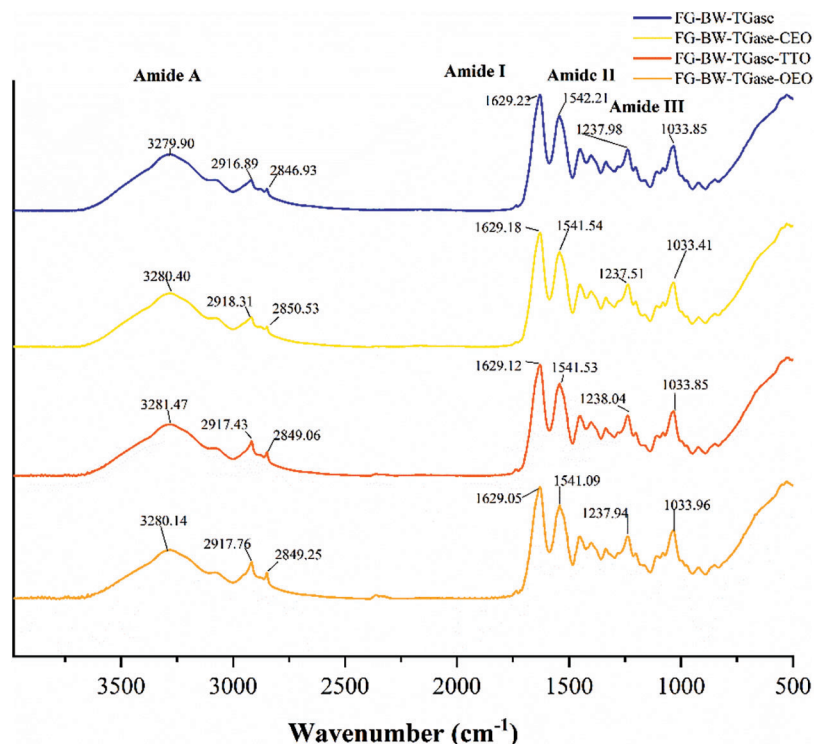


Figure 3: FTIR spectra of FG-based films

3.1.2 DSC

DSC analysis reflects the effect of essential oil incorporation on the T_m and T_g of the FG composite films. T_m indicates that the stable structure in the gelatin network is disrupted at this temperature [7]. As shown in Fig. 4a, the highest T_m of 71.86°C was obtained for the FG-BW-TGase film. The T_m of the FG-BW-TGase-CEO, FG-BW-TGase-TTO, and FG-BW-TGase-OEO films were 67.62°C, 65.97°C, and 64.48°C, respectively, indicating that the addition of EOs made the thermal stability of the gelatin films decreased [31]. EOs are small molecules that could be embedded in the gelatin network as plasticizers. Liu et al. [32] demonstrated that the addition of plasticizers to gelatin film resulted in a decrease in the film's T_m . The T_g of the films was related to the molecular structure, intermolecular interactions, and chain stiffness. As shown in Fig. 4b, the T_g values of the four films FG-BW-TGase, FG-BW-TGase-CEO, FG-BW-TGase-TTO, and FG-BW-TGase-OEO were 116.36°C, 108.24°C, 113.65°C, and 104.25°C, respectively. The T_g of the films decreased with the addition of EOs, indicating that the initially rigid films became relatively flexible and supple, consistent with the results of the mechanical properties of the films.

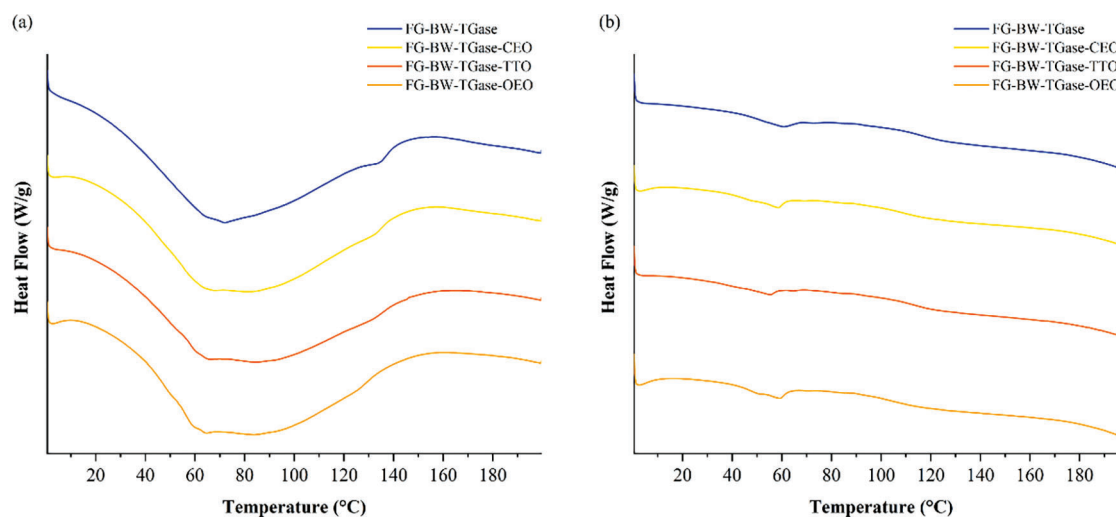


Figure 4: DSC profiles of FG-based films at (a) first heating-up and (b) second heating-up

3.1.3 Analysis of Mechanical Properties

The mechanical properties of the films are shown in Table 1. The TS of the FG-BW-TGase film was maximum at 9.05 MPa, and those of the FG-BW-TGase-CEO, FG-BW-TGase-TTO, and FG-BW-TGase-OEO films were 8.71, 8.64, and 8.11 MPa, respectively. Kavooosi et al. [33] similarly found that adding EOs to gelatin films decreased the film's TS. Long protein chains mainly maintain the protein structure of gelatin membranes, and adding oils and fats could hinder the interaction between long-chain proteins, resulting in a decrease in the TS of the films. In addition, differences in the components between EOs may affect the TS of the films. Silva et al. [34] investigated the effect of CEO, palm oil, and OEO on the mechanical properties of gelatin films. The addition of EO also reduced the TS of the films, and the TS of the gelatin films with OEO was lower than that of the samples with CEO and palm oil. Meanwhile, the EAB of the films containing EOs increased by 23.18%–29.67% ($p < 0.05$) compared with that of FG-BW-TGase, implying better flexibility of the films in the experimental group. The EOs penetrated the protein molecular chains and weakened the polymer interactions, thus increasing the flexibility and elongation of the films.

Table 1: Mechanical properties of FG-based films

Film	TS (MPa)	EAB (%)
FG-BW-TGase	9.05 ± 0.48 ^b	167.13 ± 21.78 ^a
FG-BW-TGase-CEO	8.71 ± 0.41 ^b	190.31 ± 11.64 ^b
FG-BW-TGase-TTO	8.64 ± 0.38 ^b	191.90 ± 22.41 ^b
FG-BW-TGase-OEO	8.11 ± 0.49 ^a	196.80 ± 27.46 ^b

Note: Different superscript letters in the same column indicate significant differences ($p < 0.05$).

3.1.4 Analysis of Barrier Properties

The barrier properties of a film are an essential measure of its quality because they could prevent the transfer of food deterioration factors, such as moisture and oxygen, between the environment and the food [34]. As shown in Table 2, the WVP of the composite films ranged between 1.19×10^{-11} and $1.26 \times 10^{-11} \text{ g}\cdot\text{m}^{-1}\cdot\text{s}^{-1}\cdot\text{Pa}^{-1}$. It is generally believed that EOs are hydrophobic and can react with the

polar groups in the gelatin side chains to reduce the water binding sites in the film, thus reducing the WVP [30]. In this study, the addition of EOs did not significantly reduce the WVP of the films ($p > 0.05$). The WVP is not dependent on a sole factor, it is the result of a complex combination of factors, such as film structure, composition, additives, and environment.

Table 2: The WVP and OTR of FG-based films

Film	WVP ($\times 10^{-11} \text{ g}\cdot\text{m}^{-1}\cdot\text{s}^{-1}\cdot\text{Pa}^{-1}$)	OTR ($\text{cm}^3\cdot\text{m}^{-2}\cdot 24\text{h}^{-1}\cdot 0.1\text{MPa}^{-1}$)
FG-BW-TGase	1.26 ± 0.03^a	78.50 ± 17.23^a
FG-BW-TGase-CEO	1.19 ± 0.07^a	139.07 ± 14.85^b
FG-BW-TGase-TTO	1.20 ± 0.21^a	107.30 ± 12.75^{ab}
FG-BW-TGase-OEO	1.20 ± 0.08^a	104.33 ± 23.32^a

Note: Different superscript letters in the same column indicate significant differences ($p < 0.05$).

The OTR of the FG-BW-TGase films was $78.50 \text{ cm}^3\cdot\text{m}^{-2}\cdot 24 \text{ h}^{-1}\cdot 0.1 \text{ MPa}^{-1}$. The OTRs of the FG-BW-TGase-CEO, FG-BW-TGase-TTO, and FG-BW-TGase-OEO films were 139.07, 107.30, and $104.33 \text{ cm}^3\cdot\text{m}^{-2}\cdot 24 \text{ h}^{-1}\cdot 0.1 \text{ MPa}^{-1}$. Silva et al. [34] similarly found that adding trans-cinnamaldehyde significantly affected the OTR of PLA/PBAT composite films. EOs affected the orientation and homogeneity of the polymer network and increased the pores in the polymeric film matrix, which led to an increase in the OTR of the active films. In addition, oxygen was found to be more easily transported in low-polarity EOs [35].

3.1.5 MC, WS, and WCA of Films

MC is commonly used to indicate the film matrix's total free volume of water molecules. As shown in Table 3, the highest MC was found for the FG-BW-TGase film with 22.24%. The addition CEO, TTO, and OEO reduced the MC of the films ($p > 0.05$), which may be attributed to the incorporation of hydrophobic EOs in the hydrophilic gelatin matrix that could weaken the interaction between water and biopolymer functional groups [36].

Table 3: The MC, WS, and WCA of FG-based films

Film	MC (%)	WS (%)	WCA ($^\circ$)	Image
FG-BW-TGase	22.24 ± 1.98^a	21.99 ± 7.79^a	56.72 ± 6.01^a	
FG-BW-TGase-CEO	18.20 ± 0.80^a	21.27 ± 3.48^a	77.39 ± 4.68^b	
FG-BW-TGase-TTO	18.48 ± 3.41^a	19.30 ± 2.47^a	69.73 ± 12.30^{ab}	
FG-BW-TGase-OEO	17.59 ± 2.30^a	23.91 ± 2.48^a	74.49 ± 6.91^{ab}	

Note: Different superscript letters in the same column indicate significant differences ($p < 0.05$).

Gelatin is a water-soluble substance that partially dissolves when it comes in contact with water and loses its fibrous structure [34]. As shown in Table 3, the WS of the four groups of films ranged from 19.30% to 23.91%. For active gelatin films, appropriate WS is more conducive to releasing active substances, thus prolonging the shelf life of food products. Wu et al. [37] demonstrated a reduction in the total aerobic plate count and total volatile basic nitrogen values of fish samples when wrapped in a gelatin-chitosan-OEO composite film with a WS of 30.16%.

The WCA value is often used to indicate the water sensitivity of the film surface. As shown in Table 3, the WCA value of the FG-BW-TGase film was 56.72% because the primary raw materials used in the film, such as gelatin and glycerol, are hydrophilic substances. The addition of CEO, TTO, and OEO increased the WCA of the films to 77.39%, 69.73%, and 74.49%, respectively, may be due to the volatile effect of EOs to form a hydrophobic layer on the surface of the films, thus increasing the WCA value of the films [38].

3.1.6 Antioxidant Properties of Gelatin-Based Active Films

As shown in Fig. 5, the FG-BW-TGase film had a 14.15% DPPH free radical scavenging ability, which is consistent with the study of Li et al. [38]. The peptides obtained from gelatin enzymatic digestion were able to inhibit lipid peroxidation, scavenge free radicals, and chelate metal ions. The antioxidant capacity of these peptides is related to their amino acid composition and molecular structure [39]. In general, EOs are considered to be an excellent source of antioxidants. The FG-BW-TGase-CEO film achieved the highest DPPH free radical scavenging rate of 39.38% ($p > 0.05$), followed by film added with OEO and TTO with DPPH radical scavenging rates of 31.28% and 23.01%. A study by Silva et al. [34] similarly confirmed that the antioxidant activity of CEO was higher than that of palm oil and OEO. The antioxidant ability of EOs is closely related to their composition. For CEO, components such as eugenol, sphagnum, and eugenol acetate have excellent antioxidant properties. In addition, the film matrix and interaction between the EOs and film matrix may ultimately affect the overall antioxidant properties of the film [23].

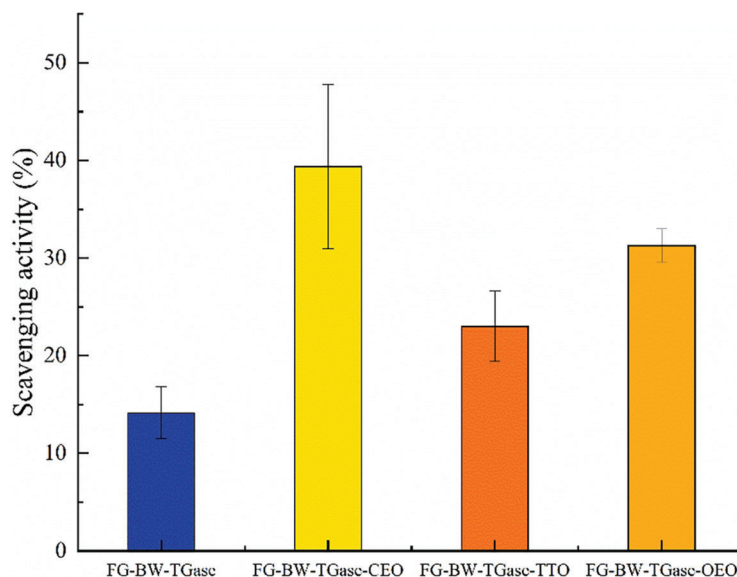


Figure 5: Comparison of DPPH radical scavenging ability of FG-based films

3.1.7 Antibacterial Properties of Gelatin-Based Active Films

Gram-positive bacterium *S. aureus* and Gram-negative bacterium *E. coli* were used as experimental subjects to investigate the antibacterial properties of the active gelatin films loaded with EOs. As shown

in Fig. 6, all three groups of active films showed some antibacterial activity against both bacteria. The EOs could disrupt the cell wall and cytoplasmic membrane of pathogenic bacteria, causing cytoplasmic leakage and eventually leading to bacterial death [11,40]. The FG-BW-TGase-OEO film showed the most robust bacterial inhibition against *S. aureus* and *E. coli*, with 98.84% and 99.86%, respectively (Table S1). Phenolic compounds, such as carvacrol and thymol, are OEO's most important active substances with significant antibacterial activity. Silva et al. [34] compared the antibacterial activity of CEO, palm essential oil, and OEOs by inhibition circle size, and the results showed that OEO films had the highest inhibition activity, with inhibition circle sizes of 14.1 and 11.73 mm for *E. coli* and *S. aureus*, respectively.

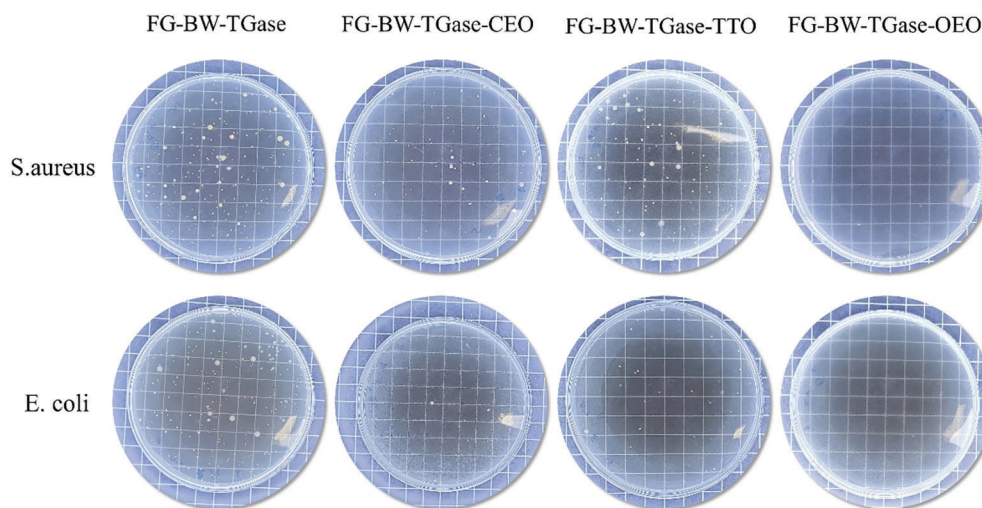


Figure 6: Comparison of FG-based films for the inhibition ability against *S. aureus* and *E. coli*

3.2 Bread Preservation

3.2.1 Water Distribution in Bread

Low-field nuclear magnetic resonance (LF-NMR) has been an emerging technique for water state analysis in recent years. In LF-NMR, a stable reaction signal exists between hydrogen protons and the sample, and the relaxation time obtained by measuring the signal change could be used to describe the state of existence of water molecules [41]. The length of the relaxation time could reflect the binding relationship between water and matter; the shorter the relaxation time, the lower the degree of freedom of the proton and the tighter the binding of water to matter, and vice versa. As shown in Fig. 7, three peaks in all the bread samples, from left to right, correspond to the relaxation times T_{21} , T_{22} , and T_{23} of the samples. T_{21} stands for bound water, mainly bound to protein molecules by chemical forces, T_{22} stands for non-fluidizable water that is bounded inside a dense spatial network structure, and T_{23} mainly refers to the free water that is free to flow outside the spatial structure of the bread [42]. As seen in Fig. 6, all bread groups showed different degrees of reduction in non-fluidizable water during storage. The recrystallization of starch led to the dissociation of water adsorbed in the bread fibers, resulting in a decrease in the amount of non-fluidizable water in the bread. The faster water loss in the gelatin film-wrapped bread samples than that in the PE group bread samples was related to the strong water absorption capacity of the protein network in gelatin. In addition, the humidity difference between the inside and outside environment of the package resulted in the continuous diffusion of water from the bread to the outside environment.

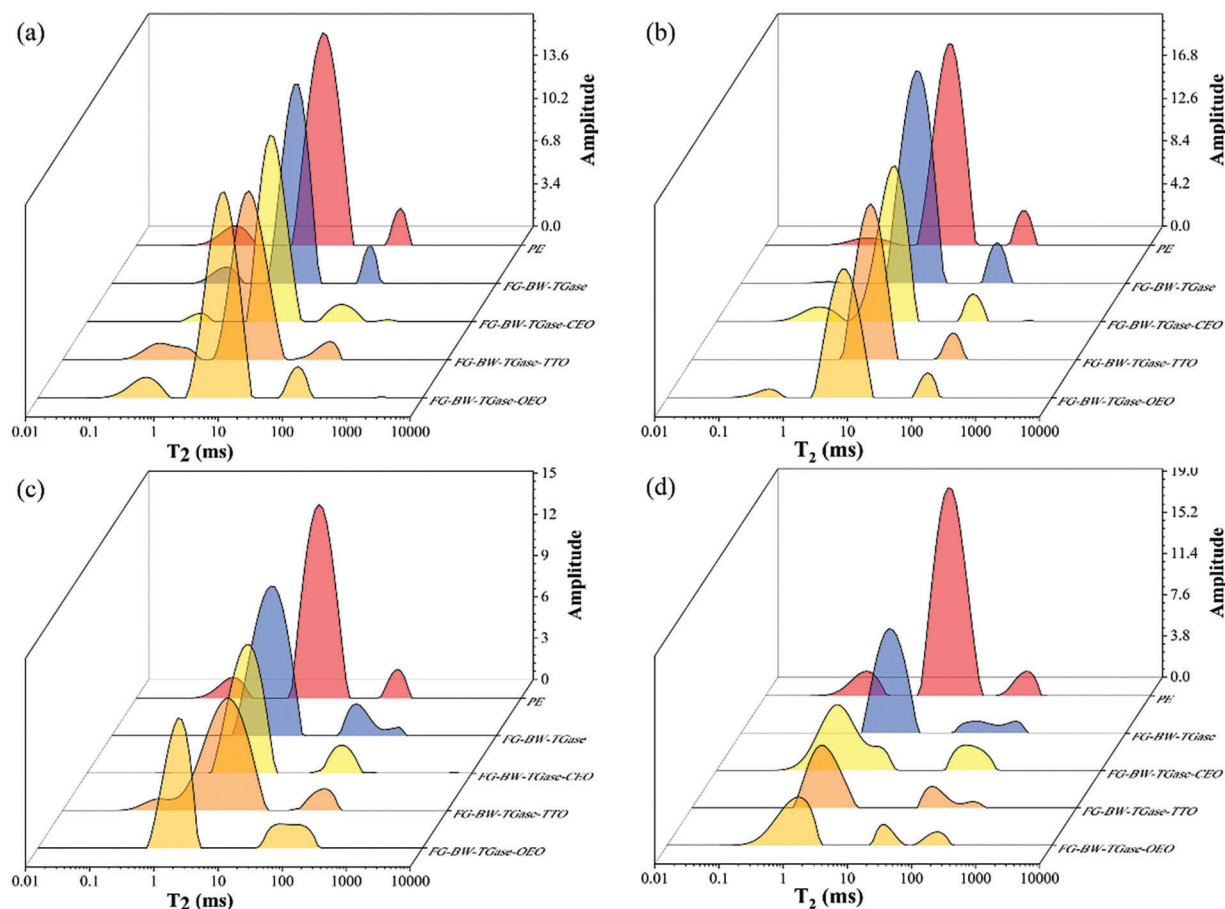


Figure 7: LF-NMR changes in bread samples preserved by different films during storage. (a)–(d) represent 1, 3, 5, and 7 days, respectively

3.2.2 Textural Changes in Bread

The bread's texture strongly depended on the plasticizing effect of water. As shown in Fig. 8, the hardness of all bread samples increased continuously with storage time, resulting from the starch recrystallization process that accelerated the release of adsorbed water and increased the hardness of the bread. In addition, the vapor pressure gradient in the microenvironment inside the package caused continuous water loss from the bread, and the water permeability of the film contributed to the water loss from the bread samples. The variation in hardness of the bread samples preserved by the gelatin film was greater, mainly due to the water absorption of gelatin itself, which increased the water loss from the bread. In addition, the bread preserved in active gelatin films tended to demonstrate higher hardness than that preserved in blank gelatin films. Srisa et al. [27] also found that bread samples preserved by active PLA/PBAT films containing trans-formaldehyde tended to have higher hardness. This finding may be due to the interaction between the active substances released in the film and the starch and proteins, resulting in a plasticized bread matrix that is more susceptible to losing previously adsorbed water.

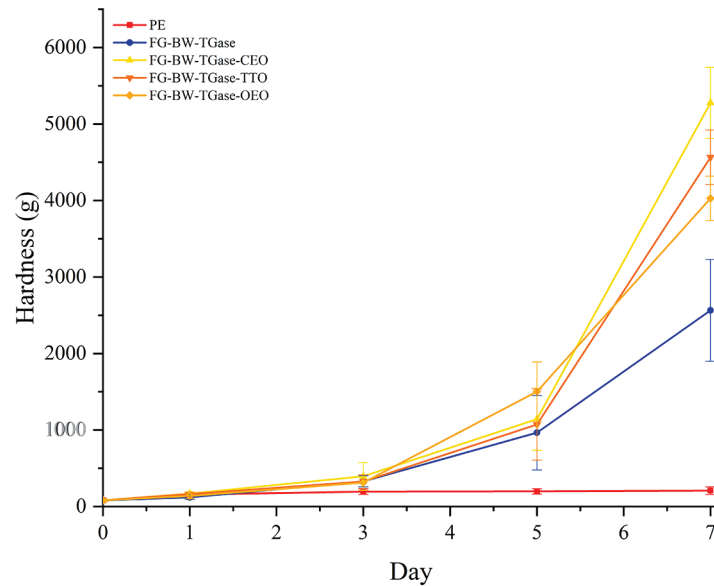


Figure 8: Changes in the texture of bread samples preserved by different films during storage

3.2.3 Microbial Changes in Bread

As shown in Fig. 9, the TVC, yeast and mold colony counts of fresh bread were 1.87 and 0.06 log CFU/g, respectively. The TVC and yeast and mold colony counts of the PE film-preserved bread samples were 6.76 and 3.92 log CFU/g, respectively, on the third day of storage, when mold spots had grown on the surface of the bread (Fig. S1). The shelf life of bread may be affected by the package’s barrier and the food’s nutritional components. The bread samples preserved in PE film had a softer texture and a higher moisture content than the other groups, and this phenomenon is more conducive to microbial growth and reproduction. The total colony count, yeast and mold colony count of the bread samples preserved by the FG-BW-TGase film were 5.94 and 4.93 log CFU/g, respectively, on the fifth day, when the mold spots were visible to the naked eye on the surface of the bread (Fig. S1). The growth of microorganisms was significantly inhibited by adding EOs ($p < 0.05$). No significant difference ($p > 0.05$) was found in the microbial inhibition ability of the different active gelatin films during bread preservation, all of them showed mold on the surface of the bread on the seventh day (Fig. S1).

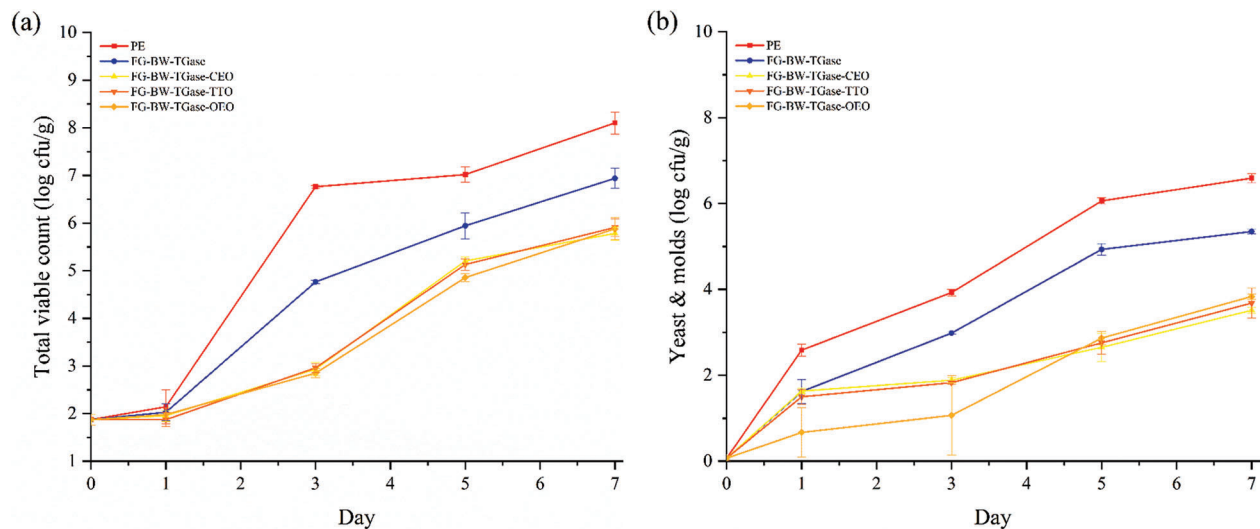


Figure 9: Changes in (a) total viable counts and (b) yeast and molds of bread samples preserved by different films during storage

4 Conclusions

In this study, FG-based active films were prepared by melt extrusion method, which significantly improved the production efficiency of active films. EOs, as small molecules, could be embedded in the gelatin network to plasticize the gelatin films, making the prepared gelatin films more flexible and elastic. The addition of EOs increased the bioactivity of the gelatin films. In the antibacterial test of the films, the FG active films showed good antibacterial properties against *S. aureus* and *E. coli*. The protein network in the FG films exhibited some water absorption properties, which may affect the texture of the preserved food. However, the bread samples preserved by PE film started to show mold on the surface of the bread on the third day of storage. Meanwhile, the bread samples preserved by the activated gelatin film showed mold visible to the naked eye on the seventh day, thereby proving the FG active film's potential for extending the baked goods' shelf life. The films prepared by melt extrusion of fish gelatin particles extracted from fish processing by-products showed good packaging performance, demonstrating their market prospect and application potential in partly replacing traditional commercial plastic packaging.

Funding Statement: The project was supported by the Program of Shanghai Tobacco Group Open Fund (20210105).

Conflicts of Interest: The authors declare that they have no conflicts of interest to report regarding the present study.

References

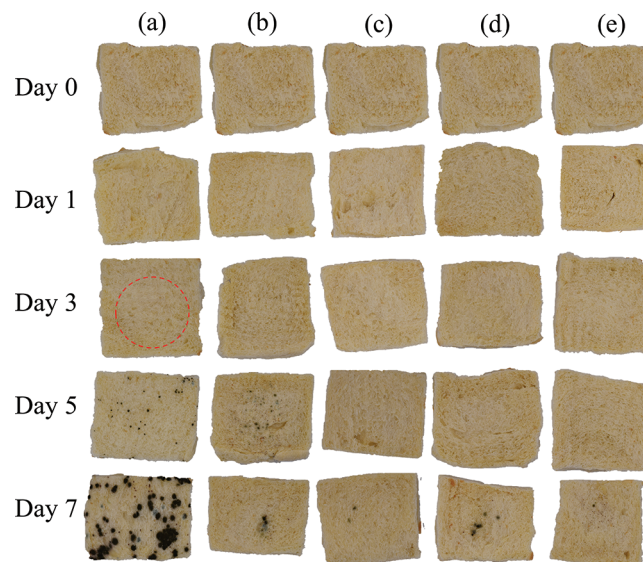
1. Jogi, K., Bhat, R. (2020). Valorization of food processing wastes and by-products for bioplastic production. *Sustainable Chemistry and Pharmacy*, 18(1), 100326. <https://doi.org/10.1016/j.scp.2020.100326>
2. He, X., Li, M., Gong, X. C., Niu, B. L., Li, W. F. (2021). Biodegradable and antimicrobial CSC films containing cinnamon essential oil for preservation applications. *Food Packaging and Shelf Life*, 29, 100697. <https://doi.org/10.1016/j.fpsl.2021.100697>
3. Huang, T., Tu, Z. C., Shangguan, X. C., Sha, X. M., Wang, H. et al. (2019). Fish gelatin modifications: A comprehensive review. *Trends in Food Science & Technology*, 86(5), 260–269. <https://doi.org/10.1016/j.tifs.2019.02.048>
4. Kaynarca, G. B., Guemues, T., Kamer, D. D. A. (2022). Rheological properties of fish (*Sparus aurata*) skin gelatin modified by agricultural wastes extracts. *Food Chemistry*, 393(1), 133348. <https://doi.org/10.1016/j.foodchem.2022.133348>
5. Gómez-Guillén, M. C., Pérez-Mateos, M., Gómez-Estaca, J., López-Caballero, E., Giménez, B. et al. (2009). Fish gelatin: A renewable material for developing active biodegradable films. *Trends in Food Science & Technology*, 20(1), 3–16. <https://doi.org/10.1016/j.tifs.2008.10.002>
6. Lv, L. C., Huang, Q. Y., Ding, W., Xiao, X. H., Zhang, H. Y. et al. (2019). Fish gelatin: The novel potential applications. *Journal of Functional Foods*, 63, 103581.
7. Zheng, H., Zhao, M. Y., Dong, Q. F., Fan, M., Wang, L. et al. (2022). Extruded transglutaminase-modified gelatin-beeswax composite packaging film. *Food Hydrocolloids*, 132, 107849.
8. Hadidi, M., Pouramin, S., Adinepour, F., Haghani, S., Jafari, S. M. (2020). Chitosan nanoparticles loaded with clove essential oil: Characterization, antioxidant and antibacterial activities. *Carbohydrate Polymers*, 236, 116075.
9. Liu, X. L., Zhang, C. H., Liu, S. C., Gao, J. L., Cui, T. E. et al. (2020). Coating white shrimp (*Litopenaeus vannamei*) with edible fully deacetylated chitosan incorporated with clove essential oil and kojic acid improves preservation during cold storage. *International Journal of Biological Macromolecules*, 162, 1276–1282.
10. Yang, Z. K., Li, M. R., Zhai, X. D., Zhao, L., Tahir, H. E. et al. (2022). Development and characterization of sodium alginate/tea tree essential oil nanoemulsion active film containing TiO₂ nanoparticles for banana packaging. *International Journal of Biological Macromolecules*, 213, 145–154.

11. Hao, Y. P., Kang, J. M., Yang, R., Li, H., Cui, H. X. et al. (2022). Multidimensional exploration of essential oils generated via eight oregano cultivars: Compositions, chemodiversities, and antibacterial capacities. *Food Chemistry*, 374(4), 131629. <https://doi.org/10.1016/j.foodchem.2021.131629>
12. Yang, C. X., Tang, H. B., Wang, Y. F., Liu, Y., Wang, J. et al. (2019). Development of PLA-PBSA based biodegradable active film and its application to salmon slices. *Food Packaging and Shelf Life*, 22(1), 100393. <https://doi.org/10.1016/j.fpsl.2019.100393>
13. Jin, J., Nguyen, T. T. H., Humayun, S., Park, S., Oh, H. et al. (2021). Characteristics of sourdough bread fermented with *Pediococcus pentosaceus* and *Saccharomyces cerevisiae* and its bio-preservative effect against *Aspergillus flavus*. *Food Chemistry*, 345(16), 128787. <https://doi.org/10.1016/j.foodchem.2020.128787>
14. Clemente, I., Aznar, M., Nerin, C. (2019). Synergistic properties of mustard and cinnamon essential oils for the inactivation of foodborne moulds *in vitro* and on Spanish bread. *International Journal of Food Microbiology*, 298(1), 44–50. <https://doi.org/10.1016/j.ijfoodmicro.2019.03.012>
15. Qian, M. Y., Liu, D. H., Zhang, X. H., Yin, Z. P., Ismail, B. B. et al. (2021). A review of active packaging in bakery products: Applications and future trends. *Trends in Food Science & Technology*, 114, 459–471. <https://doi.org/10.1016/j.tifs.2021.06.009>
16. Nilswan, K., Guerrero, P., Caba, K., Benjakul, S., Prodpran, T. (2019). Properties of fish gelatin films containing epigallocatechin gallate fabricated by thermo-compression molding. *Food Hydrocolloids*, 97(4), 105236. <https://doi.org/10.1016/j.foodhyd.2019.105236>
17. Ahammed, S., Liu, F., Wu, J., Khin, M. N., Yokoyama, W. H. et al. (2021). Effect of transglutaminase crosslinking on solubility property and mechanical strength of gelatin-zein composite films. *Food Hydrocolloids*, 116(4), 106649. <https://doi.org/10.1016/j.foodhyd.2021.106649>
18. ASTM (2012). Standard test method for tensile properties of thin plastic sheeting. Standards designations: D882-12.
19. ASTM (2015). Standard Test method for determining gas permeability characteristics of plastic film and sheeting. Standards designations: D1434-82.
20. Jiang, J. Y., Gong, L., Dong, Q. F., Kang, Y. F., Osako, K. et al. (2020). Characterization of PLA-P3,4HB active film incorporated with essential oil: Application in peach preservation. *Food Chemistry*, 313(2), 126134. <https://doi.org/10.1016/j.foodchem.2019.126134>
21. ASTM (2016). Standard test methods for water vapor transmission of materials. Standards designations: E96/E96M-16.
22. Chen, J. W., Li, Y. X., Shi, W. Z., Zheng, H., Wang, L. et al. (2021). Release of cinnamaldehyde and thymol from PLA/Tilapia fish Gelatin-Sodium alginate bilayer films to liquid and solid food simulants, and Japanese sea bass: A comparative study. *Molecules*, 26(23), 7140. <https://doi.org/10.3390/molecules26237140>
23. Liu, Z., Lin, D. H., Li, N., Yang, X. B. (2022). Characterization of konjac glucomannan-based active films loaded with thyme essential oil: Effects of loading approaches. *Food Hydrocolloids*, 124(7), 107330. <https://doi.org/10.1016/j.foodhyd.2021.107330>
24. Cui, H. Y., Siva, S., Lin, L. (2019). Ultrasound processed cuminaldehyde/2-hydroxypropyl-beta-cyclodextrin inclusion complex: Preparation, characterization and antibacterial activity. *Ultrasonics Sonochemistry*, 56, 84–93.
25. Zhou, Q., Li, P., Fang, S., Mei, J., Xie, J. (2020). Preservative effects of gelatin active coating containing eugenol and higher CO₂ concentration modified atmosphere packaging on Chinese sea bass (*Lateolabrax maculatus*) during superchilling (−0.9 °C) storage. *Molecules*, 25(4), 25040871. <https://doi.org/10.3390/molecules25040871>
26. Ju, J., Xie, Y. F., Yu, H., Guo, Y. H., Cheng, Y. L. et al. (2020). A novel method to prolong bread shelf life: Sachets containing essential oils components. *LWT*, 131(2), 109744. <https://doi.org/10.1016/j.lwt.2020.109744>
27. Srisa, A., Harnkarnsujarit, N. (2020). Antifungal films from trans-cinnamaldehyde incorporated poly(lactic acid) and poly(butylene adipate-co-terephthalate) for bread packaging. *Food Chemistry*, 333(9), 127537. <https://doi.org/10.1016/j.foodchem.2020.127537>
28. Filho, J. G. D. O., Bezerra, C. C. D. O. N., Albiero, B. R., Oldoni, F. C. A., Miranda, M. et al. (2020). New approach in the development of edible films: The use of carnauba wax micro- or nanoemulsions in arrowroot starch-based films. *Food Packaging and Shelf Life*, 26(6), 100589. <https://doi.org/10.1016/j.fpsl.2020.100589>

29. Nunez-Flores, R., Gimenez, B., Fernandez-Martin, F., Lopez-Caballero, M. E., Montero, M. P. et al. (2013). Physical and functional characterization of active fish gelatin films incorporated with lignin. *Food Hydrocolloids*, 30(1), 163–172. <https://doi.org/10.1016/j.foodhyd.2012.05.017>
30. Shankar, S., Wang, L. F., Rhim, J. W. (2019). Effect of melanin nanoparticles on the mechanical, water vapor barrier, and antioxidant properties of gelatin-based films for food packaging application. *Food Packaging and Shelf Life*, 21, 100363. <https://doi.org/10.1016/j.foodres.2019.100363>
31. Suput, D., Lazic, V., Pezo, L., Markov, S., Vastag, Z. et al. (2016). Characterization of starch edible films with different essential oils addition. *Polish Journal of Food and Nutrition Sciences*, 66(4), 277–285. <https://doi.org/10.1515/pjfn-2016-0008>
32. Liu, F., Chiou, B. S., Avena-Bustillos, R. J., Zhang, Y., Li, Y. et al. (2017). Study of combined effects of glycerol and transglutaminase on properties of gelatin films. *Food Hydrocolloids*, 65, 1–9. <https://doi.org/10.1016/j.foodhyd.2016.10.004>
33. Kavoosi, G., Rahmatollahi, A., Dadfar, S. M. M., Purfard, A. M. (2014). Effects of essential oil on the water binding capacity, physico-mechanical properties, antioxidant and antibacterial activity of gelatin films. *LWT - Food Science and Technology*, 57(2), 556–561. <https://doi.org/10.1016/j.lwt.2014.02.008>
34. Silva, N. D. E., Farias, F. D., Freitas, M. M. D., Hernandez, E. J. G. P., Dantas, V. V. et al. (2021). Artificial intelligence application for classification and selection of fish gelatin packaging film produced with incorporation of palm oil and plant essential oils. *Food Packaging and Shelf Life*, 27(7), 100611. <https://doi.org/10.1016/j.foodres.2020.100611>
35. Perdones, A., Vargas, M., Atares, L., Chiralt, A. (2014). Physical, antioxidant and antimicrobial properties of chitosan-cinnamon leaf oil films as affected by oleic acid. *Food Hydrocolloids*, 36(9–10), 256–264. <https://doi.org/10.1016/j.foodhyd.2013.10.003>
36. Vianna, T. C., Marinho, C. O., Marangoni, L., Ibrahim, S. A., Vieira, R. P. (2021). Essential oils as additives in active starch-based food packaging films: A review. *International Journal of Biological Macromolecules*, 182, 1803–1819. <https://doi.org/10.1016/j.ijbiomac.2021.05.170>
37. Wu, J., Ge, S., Liu, H., Wang, S., Chen, S. et al. (2014). Properties and antimicrobial activity of silver carp (*Hypophthalmichthys molitrix*) skin gelatin-chitosan films incorporated with oregano essential oil for fish preservation. *Food Packaging and Shelf Life*, 2(1), 7–16. <https://doi.org/10.1016/j.foodres.2014.04.004>
38. Li, Y. J., Tang, C. M., He, Q. F. (2021). Effect of orange (*Citrus sinensis* L.) peel essential oil on characteristics of blend films based on chitosan and fish skin gelatin. *Food Bioscience*, 41(2), 100927. <https://doi.org/10.1016/j.foodres.2021.100927>
39. Gomez-Guillen, M. C., Ihl, M., Bifani, V., Silva, A., Montero, P. (2007). Edible films made from tuna-fish gelatin with antioxidant extracts of two different murta ecotypes leaves (*Ugni molinae* Turcz). *Food Hydrocolloids*, 21(7), 1133–1143. <https://doi.org/10.1016/j.foodhyd.2006.08.006>
40. Yang, Z. H., He, Q., Ismail, B. B., Hu, Y. Q., Guo, M. M. (2022). Ultrasonication induced nano-emulsification of thyme essential oil: Optimization and antibacterial mechanism against *Escherichia coli*. *Food Control*, 133(5), 108609. <https://doi.org/10.1016/j.foodcont.2021.108609>
41. Huang, L. L., Cheng, S. S., Song, Y., Xia, K. X., Xu, X. B. et al. (2017). Non-destructive analysis of caviar compositions using low-field nuclear magnetic resonance technique. *Journal of Food Measurement and Characterization*, 11(2), 621–628. <https://doi.org/10.1007/s11694-016-9431-z>
42. Xu, F. F., Jin, X., Zhang, L., Chen, X. D. (2017). Investigation on water status and distribution in broccoli and the effects of drying on water status using NMR and MRI methods. *Food Research International*, 96(18), 191–197. <https://doi.org/10.1016/j.foodres.2017.03.041>

Appendix**Table S1:** Antibacterial rate of gelatin-based active films containing different essential oils

Film	$X_{S. aureus}$ (%)	$X_{E. coli}$ (%)
FG-BW-TGase-CEO	75.87 ± 1.75^b	98.50 ± 0.62^b
FG-BW-TGase-TTO	49.28 ± 1.15^a	91.69 ± 1.93^a
FG-BW-TGase-OEO	98.84 ± 0.90^c	99.86 ± 0.24^b

**Figure S1:** Pictures of bread preservation: (a)–(e) refer to PE, FG-BW-TGase, FG-BW-TGase-CEO, FG-BW-TGase-TTO, and FG-BW-TGase-OEO groups, respectively